# The correlation between the cycling efficiency, surface chemistry and morphology of Li electrodes in electrolyte solutions based on methyl formate

Yair Ein-Eli, Doron Aurbach

*Department of Chemistry, Bar-Ilan University, Ramat Gan 52900, Israel*

## Abstract

The correlation between Li-cycling efficiency, morphology and surface chemistry in methyl formate (MF) solutions have been investigated. The salt included $LiAsF_6$, $LiClO_4$, $LiBF_4$, and their mixtures. Propylene ethylene, dimethyl and diethyl carbonates, tetrahydrofuran and 1,3-dioxolane were used as co-solvents. The impact of $CO_2$ as an additive was also explored. Ex situ surface sensitive Fourier-transform infrared spectroscopy (FT-IR) and scanning electron microscopy were used in conjunction with standard electrochemical techniques. Li-cycling efficiency was measured in half-cell testing of electrodes prepared by Li deposition on copper. The Li-cycling efficiency in all MF solutions is poor due to the instability of the surface films formed on Li in this highly polar solvent. The use of $CO_2$ enabled high Li-cycling efficiency to be obtained due to an efficient passivation of $Li_2CO_3$ formed on Li when $CO_2$ was present. The performance of Li electrodes in these systems could be further optimized by the use of the appropriate co-solvents. The factors which determine the anode utility in these systems are discussed.

*Keywords:* Lithium electrodes; Methyl formate; Cycling efficiency; Surface chemistry; Morphology; Secondary lithium batteries

## 1. Introduction

One of the solvents of interest for secondary Li batteries is methyl formate (MF) since it is highly polar and its Li salt solutions are very conductive. Its low melting point enables this solvent to be used at a very wide temperature range. MF has a wider electrochemical window than ethers, alkyl carbonates or other esters ($\Delta V > 4.5$ V) and, therefore, its solutions are suitable for rechargeable Li systems with cathodes such as $Li_xCoO_2$, $L_xNiO_2$ or $Li_xMn_2O_4$ which are supposed to be higher in energy density than the more common $LiV_xO$, $LiTiS_2$ or $LiMnO_2$, because their rest potential is more than 4 V versus $Li/Li^+$. Consequently, several Li-battery researchers and developers focused their attention on this solvent, and there are reports on prototypes of rechargeable $LiCoO_2$ batteries in which electrolyte solutions based on MF [1] or MF–$CO_2$ [2] have been used. These publications suggest combinations of MF, alkyl carbonates (e.g., diethyl carbonate) [1], $CO_2$, $LiAsF_6$ and $LiBF_4$ as optimized electrolyte systems for $LiCoO_2$ batteries [2]. We intensively investigated the chemistry of Li electrodes in Li salt solutions of MF both under argon and $CO_2$ atmospheres using surface sensitive Fourier-transform infrared spectroscopy (FT-IR) [3]. It was found that the major surface species formed on Li in MF is Li formate ($HCO_2Li$) and when $CO_2$ is present $Li_2CO_3$ becomes a major surface species formed on Li in addition to Li formate. Salts such as $LiAsF_6$, $LiClO_4$, $LiBF_4$ or $LiPF_6$ are also involved in the Li-surface chemistry in solutions, and insoluble Li halides are formed in addition to the solvent or the atmospheric contaminants reduction products. There is also evidence that salt reduction products of the type $Li_xAsF_y$ [4], $L_xClO_y$ [5], $Li_xBF_y$ [6] or $L_xPF_yO_z$ [7] are also formed on Li in the above salt solutions, respectively.

We report here a study of the correlation between the surface chemistry, the morphology and the cycling efficiency (utility) of Li anodes in MF solutions containing different salts, and co-solvents such as propylene, ethylene, dimethyl and diethyl carbonates (PC, EC, DMC and DEC, respectively) and ethers (e.g., tetrahydrofuran (THF), 1,3-dioxolane (DN)). These systems were investigated under both argon and $CO_2$. The surface chemistry was investigated using ex situ FT-IR

spectroscopy. The morphology was investigated using scanning electron microscopy (SEM). An understanding of the above correlation, i.e., the way in which the solution composition affects the surface chemistry and morphology, and how both of these influence the performance of Li anodes, may provide tools for a judicious optimization of these electrolyte systems for use in high energy density rechargeable Li batteries.

## 2. Experimental

The cycling efficiency of Li electrodes in various solutions was measured in standard experiments in which Li was electrochemically deposited on copper (5 $C/cm^2$) (versus Li counter electrode), followed by discharge/charge cycling at depth-of-discharge (DOD) of 25% at practical current densities of 0.5 to 2 $mA/cm^2$, using the Maccor series 2000 battery charger. After 10 to 20 cycles, the residual Li was dissolved electrochemically and the cycling efficiency was calculated as described in Ref. [8]. SEM measurements were performed on Li electrodes after a few charge/discharge (deposition/dissolution) cycles in solutions followed by washing (pure solvent), drying and transferring to the SEM (JEOL-JSM-840) using a special transfer system [8]. FT-IR measurements were conducted both on Li and nickel electrodes, as it was found that Ni electrodes polarized to low potential ($<0.1$ V versus $Li/Li^+$) in Li salt solutions of esters, ethers and alkyl carbonates are covered with surface films similar to those formed on Li in the same solutions [3,9,10]. The spectral studies of Ni electrodes, however, are easier than those with Li electrodes since the transfer of the less-sensitive Ni electrodes from the solutions to the spectrometer is much less problematic compared with Li. In addition, the spectra obtained from Ni electrodes covered with the surface films (formed by their polarization to low potentials) are of a much better quality than those measured from Li. Li mirrors, prepared in situ in solutions as already described [6], were stored in solutions (for periods of hours, days or weeks), followed by washing, drying, protecting with KBr plates and measuring, as already reported [3,6,10] (external reflectance mode, ex situ, Nicolet 60 SXB spectrometer, 1000 interferometer scans). Ni mirrors (Goodfellow 99.9%) were polarized in solutions to low potentials ($>0.1$ V versus $Li/Li^+$, PAR potentiostat Model 173), followed by storage (1 h) at low potentials, washing, drying and measuring as already described [3,10]. The solvent and salt sources purification methods and the glove box operation have already been reported [3,6,8,10].

## 3. Results and discussion

Table 1 summarizes cycling efficiency data of Li electrodes in $LiAsF_6$, $LiClO_4$ and $LiBF_4$ solutions as well as in solutions containing mixtures of these salts, under both argon and $CO_2$ atmospheres of different pressures.

The cycling efficiency of Li electrodes in all of these solutions under 1 atm argon is poor. Increasing the argon pressure slightly increases the cycling efficiency measured, while changing the atmosphere to $CO_2$ drastically increases the Li-cycling efficiency measured. However, the Li-cycling efficiency in solutions containing both $LiAsF_6$ and $LiBF_4$ is lower than that measured in the single-salt solutions, as shown in Table 1. Li-cycling efficiency in the above solutions containing THF, EC, DEC, DMC and DN as co-solvents (even at concentrations of 90% by volume of the co-solvent) under argon is also very poor ($<40\%$). In contrast, Li electrodes in $LiAsF_6$ solutions of pure THF, PC, EC, DMC and DN measured under argon in the same testing procedure have cycling efficiencies of 90%, 85–90%, 90%, $>96\%$ and 90–95%, respectively. When the experiments with these solvent mixtures were performed under $CO_2$ atmosphere the picture changed considerably, as demonstrated in Fig. 1 which displays cycling efficiencies of Li electrodes in MF-co-solvent solutions under $CO_2$ (6 atm) as a function of the solvent composition. The information presented in this Figure may

Table 1
Cycling efficiency of Li electrodes in methyl formate solutions of various Li salts at different atmospheres (Li on Cu, 5 $C/cm^2$, 10 cycles at 25% DOD, 1 $mA/cm^2$)

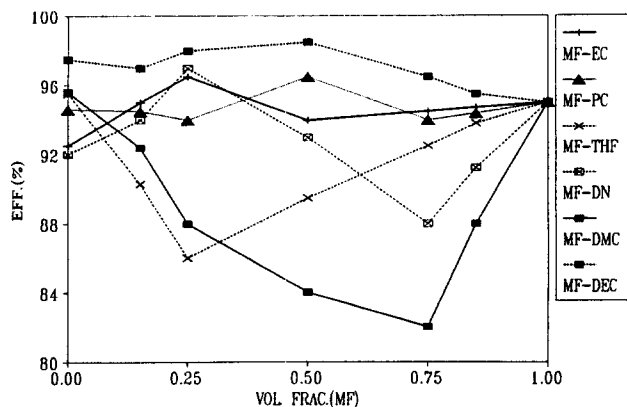| Concentration (M) | Salt | $p_{Co2}$ | $p_{Ar}$ | Efficiency (%) |
|---|---|---|---|---|
| 1 | $LiAsF_6$ | | 1 | 68 |
| | | | 7 | 80 |
| | | 3 | | 90 |
| | | 6 | | 95 |
| 1 | $LiClO_4$ | | 1 | 0 |
| | | | 7 | 70 |
| | | 3 | | 86 |
| | | 6 | | 93.5 |
| 1 | $LiBF_4$ | | 1 | 0 |
| | | 3 | | 78 |
| | | 6 | | 83 |
| 1 | $LiAsF_6$ and | | 1 | 0 |
| 1 | $LiBF_4$ | 3 | | 40 |
| | | 6 | | 60 |
| 1 | $LiAsF_6$ and | | 1 | 0 |
| 0.1 | $LiBF_4$ | 3 | | 63 |
| | | 6 | | 77 |
| 1 | $LiAsF_6$ and | 3 | | 88.5 |
| 1 | $LiClO_4$ | 6 | | 95 |

Fig. 1. Li-cycling efficiency vs. solvent composition measured in MF–LiAsF$_6$ solutions containing co-solvents as indicated, under $CO_2$ (6 atm).

be summarized as follows: the presence of $CO_2$ increases Li-cycling efficiency considerably. With PC, EC and DEC the picture is steady, in relation to the solvent ratio, with DN a minimum and maximum in Li-cycling efficiency versus MF content are obtained, and the Li-cycling efficiency measured in THF and DMC solutions of MF is lower for the mixtures than for the pure systems. Fig. 2 shows SEM micrographs obtained from Li electrodes cycled in MF–LiAsF$_6$ solutions (3 cycles: 1 C/cm$^2$ per cycle, 1 mA/cm$^2$). Fig. 2(a) relates to an experiment under argon where the last process was deposition, Fig. 2(b) and (c) relates to experiments under $CO_2$ (6 atm) where the last processes were deposition and dissolution, respectively. Fig. 2(d) and (e) is typical of Li cycled in LiAsF$_6$ solutions of MF and any alkyl carbonate (of the above list) mixture. These micrographs show that the presence of $CO_2$ has a remarkable impact on the surface morphology upon cycling. While the deposition of Li in MF–LiAsF$_6$ under $CO_2$ is dendritic, the dendrites formed are stable and dissolve completely in a consequent dissolution. This explains the high Li-cycling efficiency obtained in these systems. The morphology of Li electrodes in alkyl carbonate solutions, either pure or with MF as a co-solvent under $CO_2$ atmosphere is quite similar to that shown in Fig. 2(b) and (c). The morphology of Li electrodes in MF–THF or MF–DN solutions is quite similar to that observed in pure MF solutions. A correlation was found between the picture shown in Fig. 1 and the results obtained by SEM, as Li deposition in solution combinations in which low cycling efficiency was measured, was found to be more dendritic as compared with solutions in which high Li cycling efficiency was obtained. Fig. 3 compares the morphology of Li electrodes cycled in LiAsF$_6$ and LiAsF$_6$–LiBF$_4$ solutions in MF–DEC mixture under $CO_2$. It demonstrates that the impact of LiBF$_4$ in solutions on the Li morphology is very pronounced, which is in line with

the strong influence of this salt on the Li-cycling efficiency as presented in Table 1.

Fig. 4 shows SEM micrographs obtained from Li electrodes cycled in MF–DN (3:1) and MF–DN (1:3) solutions of 1 M LiAsF$_6$ under $CO_2$ (Fig. 4(a) and (b), respectively). At these solvent ratios, minimum and maximum in Li-cycling efficiency was measured as shown in Fig. 1. Note that Fig. 4(a) shows a highly dendritic picture, while the morphology shown in Fig. 4(b) is relatively smooth. Thus, these results correlate very well with the Li-cycling efficiency studies since dendritic deposition is one of the main causes of low Li-cycling efficiency. However, these studies obviously prove that dendrite formation alone is not the major reason for mass losses upon cycling and thus a poor cycling efficiency. The connection of the dendrites when formed to the bulk Li is also important. If the Li passivation is efficient (depending on the solution composition), electrical disconnection of these dendrites from the bulk by corrosion in their bottle necks may be largely avoided, and thus Li-cycling efficiency remains high in spite of the rough morphology. This is exactly the case of Li electrodes cycled in solutions under $CO_2$ atmosphere where the electrodes' utility is high, although their morphology is highly dendritic (Fig. 2). Fig. 5 shows an FT-IR spectrum obtained from an Ni electrode polarized in MF–THF 1 M LiAsF$_6$ solution to low potentials (as indicated). The dominant peaks in the spectrum are those of Li formate, the major MF reduction product. However, C–O peaks around 1100 to 1000 cm$^{-1}$ are also present in Fig. 5 and their source may be reduction products of THF, which are Li alkoxides [11]. Spectra obtained from Li surfaces stored in these solutions are similar to those formed on Ni at low potentials. However, those measured from Ni electrodes are of a better quality due to optical considerations and, therefore, better demonstrate the surface chemistry of these systems. Thus, these spectral studies reflect the higher reactivity of MF toward Li compared with the ethers. Nevertheless, however, ether reduction also has an impact on the Li-surface chemistry in MF–ether mixtures. This may be partly due to the fact that Li formate, the major MF reduction product on Li is more soluble in solutions than Li alkoxides. Fig. 6 shows FT-IR spectra obtained from Ni electrodes polarized to low potentials in DMC–LiAsF$_6$ and DMC–MF–LiAsF$_6$ solutions under $CO_2$ atmosphere (6 atm). The spectrum related to the single-solvent system (Fig. 6(a)) shows peaks of both ROCO$_2$Li (DMC reduction products on Li [6]) and Li$_2$CO$_3$ peaks, as indicated. Fig. 6(b) related to the solvent mixture (DMC–MF) has pronounced Li formate peaks in addition to the expected ROCO$_2$Li and Li$_2$CO$_3$ peaks. It is notable in this Fig. that when MF is present, the influence of the presence of $CO_2$ on the electrode surface chemistry decreases compared with the case of
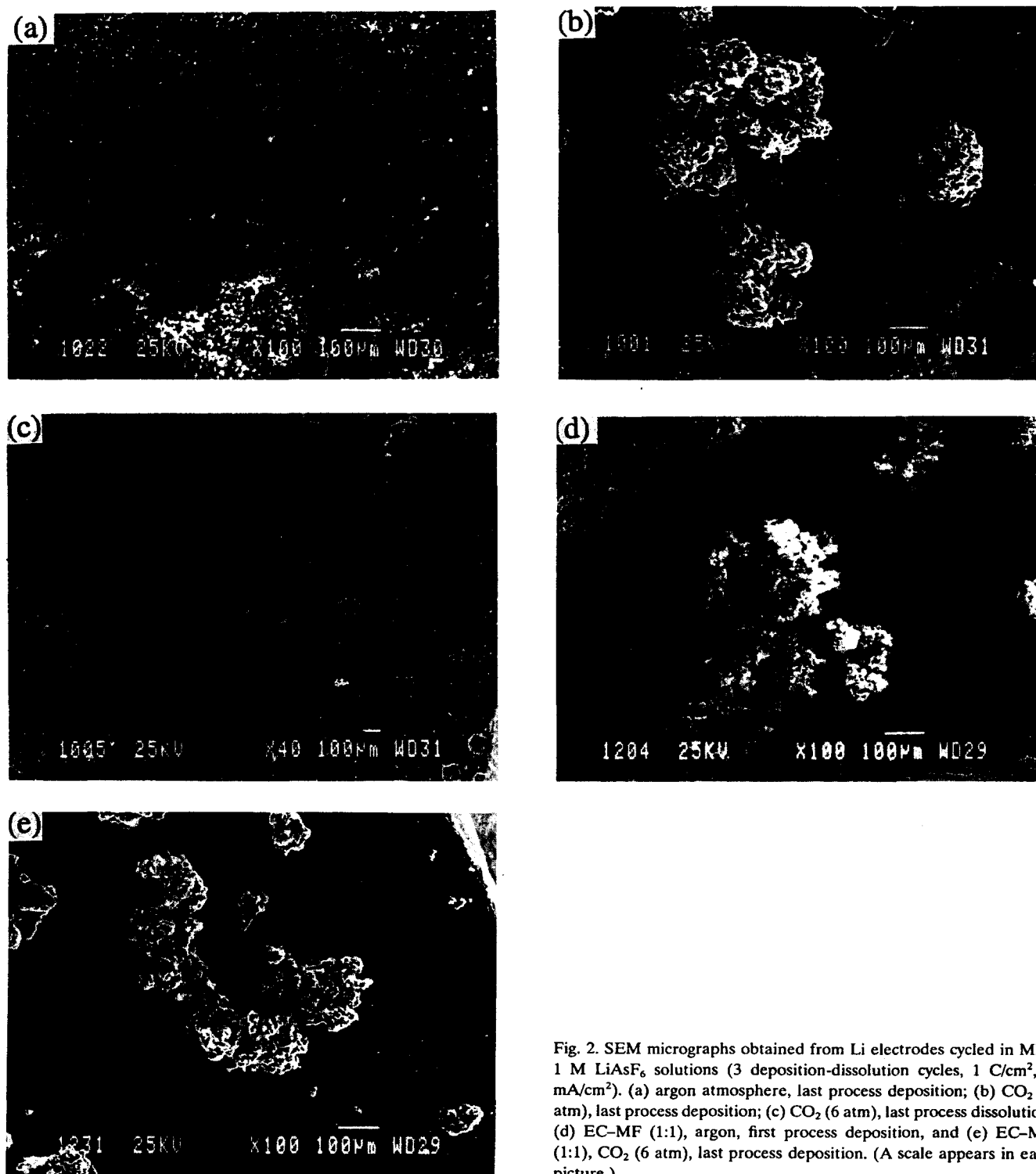
Fig. 2. SEM micrographs obtained from Li electrodes cycled in MF–1 M LiAsF$_6$ solutions (3 deposition-dissolution cycles, 1 C/cm$^2$, 1 mA/cm$^2$). (a) argon atmosphere, last process deposition; (b) CO$_2$ (6 atm), last process deposition; (c) CO$_2$ (6 atm), last process dissolution; (d) EC–MF (1:1), argon, first process deposition, and (e) EC–MF (1:1), CO$_2$ (6 atm), last process deposition. (A scale appears in each picture.)

the single-solvent system (DMC–LiAsF$_6$). This may be due to the high reactivity of MF which competes with CO$_2$ in the build-up of the surface films on Li. Fig. 7 shows FT-IR spectra obtained from Ni electrodes polarized to low potentials (20 mV versus Li/Li$^+$) in EC–MF solutions (1:1) of 1 M LiAsF$_6$ under argon and CO$_2$ atmospheres (Fig. 7(a) and (b), respectively).

Fig. 8 is a typical spectrum measured from an Li electrode stored in EC–MF (1:1) mixture with 1 M LiAsF$_6$ under argon.

In general, Fig. 8 (obtained from Li) and Fig. 7(a) (obtained from Ni) include quite similar information. These two spectra indeed demonstrate that the surface films deposited on Ni at low potentials are very similar
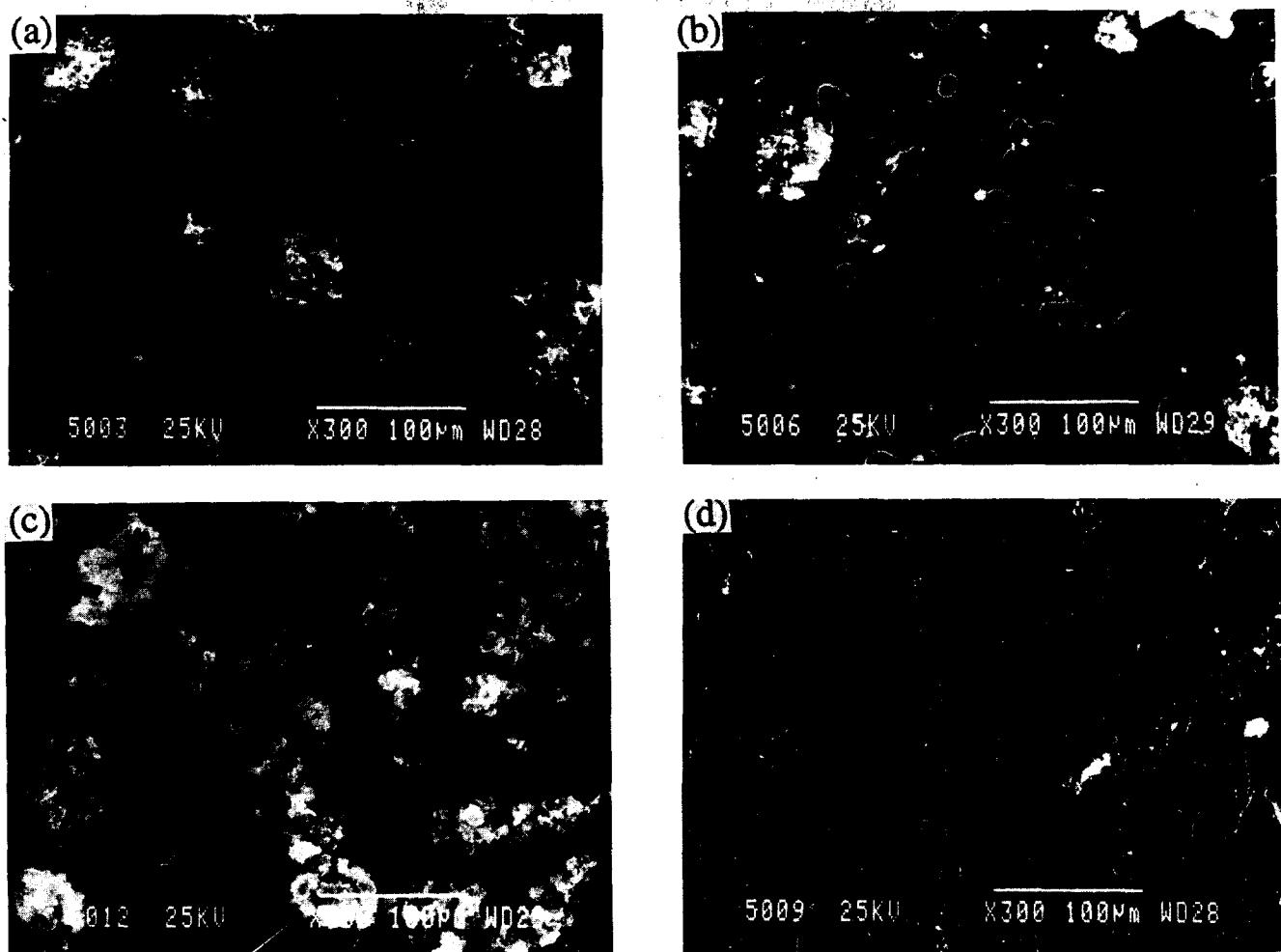
Fig. 3. SEM micrographs obtained from Li electrodes cycled (5 cycles, 1 C per process 1 mA/cm², galvanostatic) in MF–LiAsF₆ solutions under CO₂ (6 atm): (a), (b) mother solution; (c), (d) solution containing 0.2 M LiBF₄; (a), (c) last process deposition, and (b), (d) last process dissolution. (A scale appears in each picture.)

to those formed on Li in the same solutions. Thus, the use of Ni electrodes as a tool for investigating the surface chemistry of the more complicated Li electrodes is justified.

The spectral studies prove that Li electrodes in EC–MF solutions under argon are covered with surface films comprising mostly of ROCO₂Li species, probably (CH₂OCO₂Li)₂ which is the major expected EC reduction product [6], and Li formate, the major MF reduction product [3]. When CO₂ is present, Li₂CO₃ also becomes a major surface species in addition to the above solvent reduction products, as indicated in Fig. 7(b). The spectra obtained from Li or Ni electrodes treated in PC–MF mixtures under argon or CO₂ show a similar picture to that obtained with EC–MF, i.e., the surface films are composed of both PC and MF reduction products, and when CO₂ is present, Li₂CO₃ also becomes an important constituent of the surface films. This is demonstrated in Fig. 9 which shows a spectrum measured from Ni electrodes polarized to

low potentials in MF–PC–LiAsF₆ solution under CO₂. The peak assignments appearing in this Fig. are based on our previous work [3,6,10].

Fig. 10(a) shows a typical FT-IR spectrum measured ex situ from Li electrodes stored in MF–DEC–LiAsF₆ solutions. This spectrum obviously relates to a mixture of Li formate, Li alkyl carbonate (ROCO₂Li), and Li salt reduction species with As–F bonds, probably Li_xAsF_y [4]. The major surface species formed on Li in DEC solutions are CH₃CH₂OCO₂Li and CH₃CH₂OLi [12]. These species are soluble in DEC and therefore, Li dissolves in this solvent. In contrast, in MF–DEC solutions Li is quite stable, probably because of Li formate formation and a decreased solubility of DEC reduction products when MF is a co-solvent.

Fig. 10(b) relates to a similar experiment with Li stored in MF–DEC in LiAsF₆ solution containing 0.2 M LiBF₄.

As shown, the presence of this salt influences the Li surface chemistry remarkably. In addition to Li
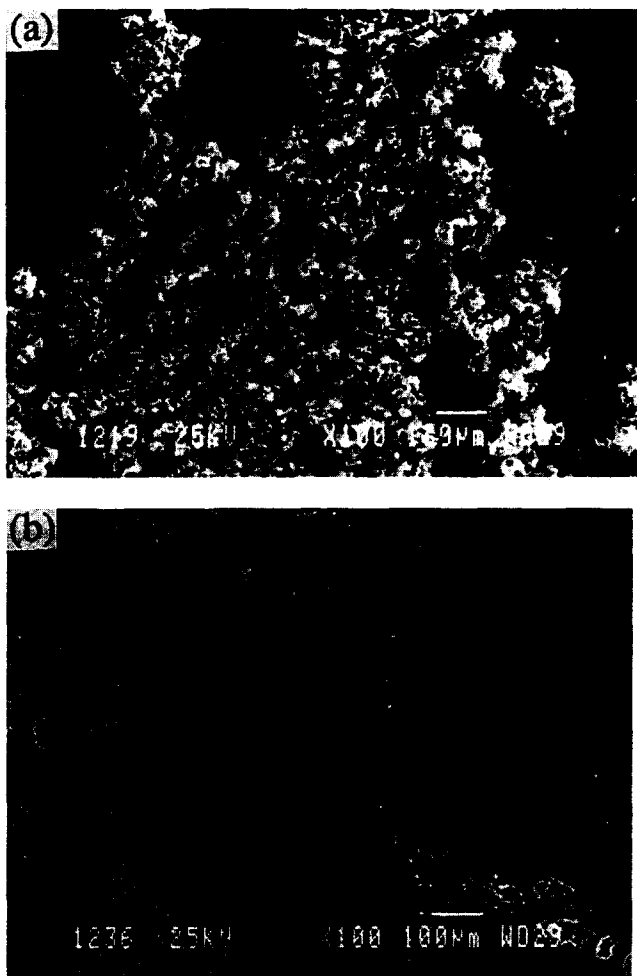
Fig. 4. SEM micrographs obtained from Li electrodes cycles (5 cycles 1 C per process 1 mA/cm$^2$, galvanostatic) in 1 M LiAsF$_6$ solutions of (a) MF–DN (3:1) and (b) MF–DN (1:3) under CO$_2$; last process deposition.
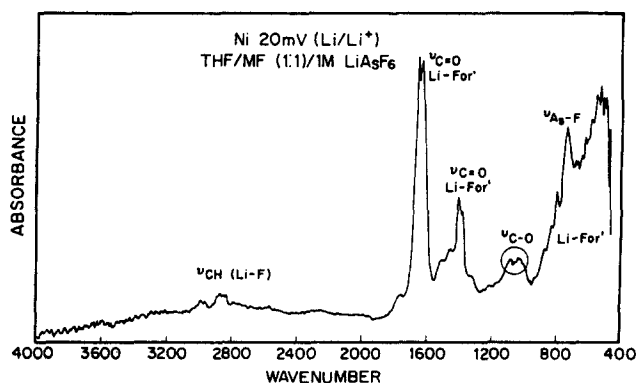


Fig. 6. FT-IR spectra obtained ex situ from Ni electrodes polarized to 20 mV vs. Li/Li$^+$ in (a) DMC–1 M LiAsF$_6$ solution and (b) DMC–MF (1:1) 1 M LiAsF$_6$ solution under CO$_2$ (6 atm). Peak assignments are based on Refs. [3,6,10].



Fig. 7. FT-IR spectra obtained ex situ from Ni electrodes polarized to 20 mV vs. Li/Li$^+$ in MF–EC (1:1) 1 M LiAsF$_6$ solutions under (a) argon and (b) 6 atm CO$_2$. Peak assignments are based on Refs. [3,10] (spectrum (a) also has residual EC peaks, as indicated).



Fig. 5. FT-IR spectra obtained ex situ (external reflectance mode) from an Ni electrode polarized to 20 mV vs. Li/Li$^+$ in MF–THF (1:1) LiAsF$_6$ solution.



Fig. 8. FT-IR spectrum obtained from an Li surface prepared in situ in MF–EC (1:1) mixture containing 1 M LiAsF$_6$ after 24 h of storage. The spectrum was obtained ex situ (external reflectance) with the Li surface protected with a KBr window.

formate and ROCO$_2$Li peaks, dominant infrared peaks attributable to boron compounds appear around 1100 to 1000 cm$^{-1}$. Despite their volatility, it was impossible
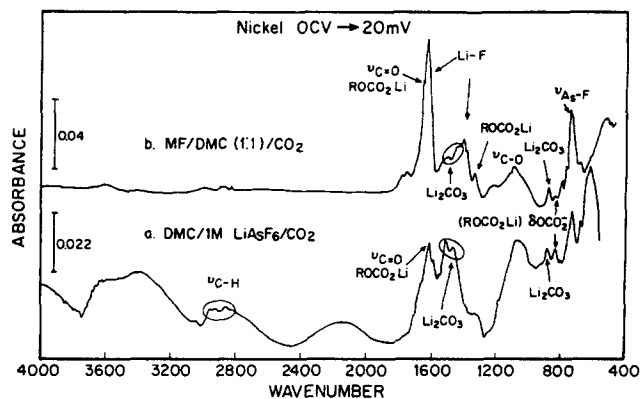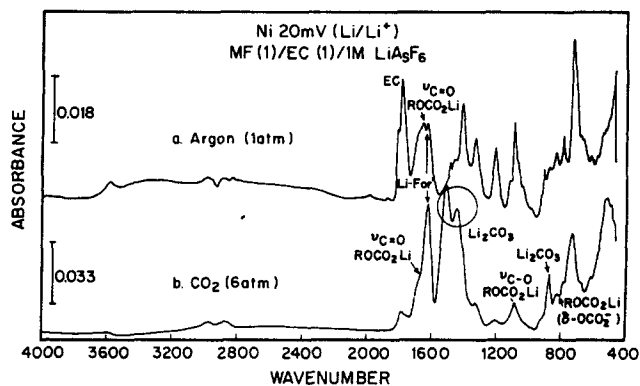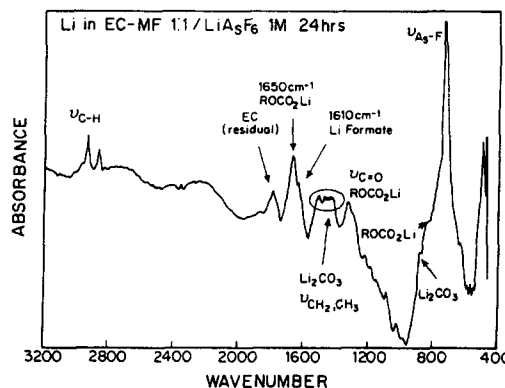
to completely dry out the solvents from the samples. This may be an indication of a formation of highly porous surface films.
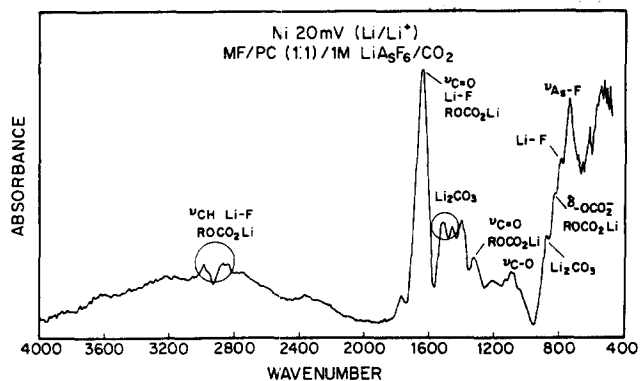
Fig. 9. FT-IR spectrum obtained ex situ from an Ni electrode polarized to 20 mV vs. $Li/Li^+$ in PC–MF (1:1) mixture containing 1 M $LiAsF_6$ under $CO_2$ (6 atm).
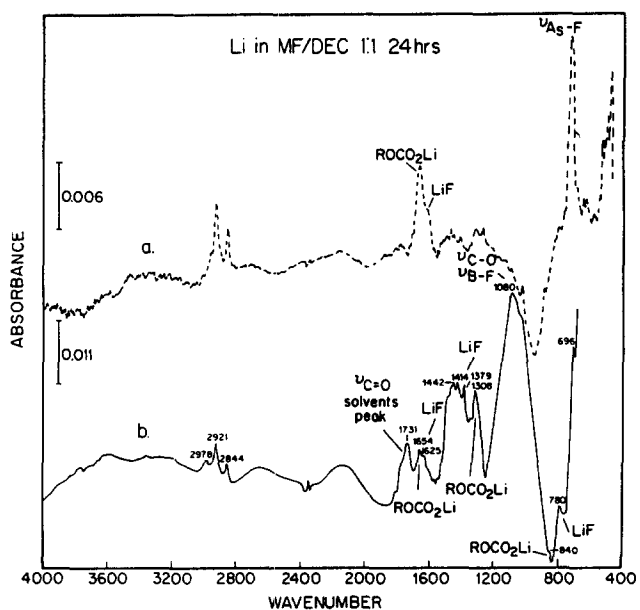


Fig. 10. FT-IR spectra obtained from Li surfaces prepared in situ in MF–DEC (1:1) mixtures containing (a) 1 M $LiAsF_6$, and (b) 1 M $LiAsF_6$, 0.2 M $LiBF_4$. The Li samples were measured spectroscopically ex situ (external reflectance) protected with KBr windows.

## 4. The correlation between the surface chemistry of Li electrodes and their cycling efficiency in solutions

The above spectral studies obviously demonstrate that the surface chemistry of Li in all of the solutions studied is determined by a delicate balance of competing reduction reactions of the solvents, salts and reactive atmospheric components (e.g., $CO_2$) on the Li surface, which precipitate insoluble organic and inorganic Li salts. The chemical composition of the Li–solution interphase is heterogeneous, containing different types of Li-ion conductors. Therefore, the electronic properties of the surface films and the Li morphology which they induced upon cycling cannot be predicted a priori since these depend on their occasional chemical com-

position. Thus, it is impossible to explain the results shown in Table 1 and Fig. 1 by simple, general rules. It can be assumed that the Li-cycling efficiency measured in this work is determined by two major factors: (i) to what extent the surface films formed in each system induce smooth and uniform Li dissolution and deposition, and (ii) to what extent are dendrites efficiently passivated by the surface films when they are formed. It should be emphasized that the correlation of the Li-cycling efficiency measured in half-cell testing and short experiments in a large volume of electrolyte solutions to the cycle life of practical batteries (utilizing the same solutions) is not simple. In a typical practical Li battery, Li electrodes are pressed to the separator leaving a very small volume of electrolyte solution in-between. In this configuration the pressure on the Li electrodes considerably suppresses dendrites formation and their disconnection from the bulk upon cycling [13,14]. It is therefore assumed that the cycling efficiency of Li electrodes in practical batteries containing the above solutions should be much higher than that measured in this work.

This explains some discrepancies between the low values of Li-cycling efficiency measured in this work in solutions of $LiBF_4$ and results obtained by others in real cell configurations [1,2] (much higher Li-cycling efficiencies). However, the short half-cell testing procedure used in this work obviously forms a very good basis for a comparison of the various electrolyte solutions. Thus, it is assumed that the trend in the Li-cycling efficiency measured in the various electrolyte systems presented in Table 1 and Fig. 1 should be clearly shown in long-term cycle-life testing of practical Li batteries.

In the absence of $CO_2$, Li-cycling efficiency measured in all MF solutions is very low. This should be attributed to the fact that this solvent is highly polar and reactive. Most of the surface species formed in the above systems are mostly organic Li salts and partly soluble, and therefore the Li passivation is poor. When $CO_2$ is present, $Li_2CO_3$ is formed, which is supposed to have the lowest solubility product than any other major surface species formed by solvent reduction. Therefore, it is an excellent passivating agent. The variations shown in the Li-cycling efficiency values as a function of the solvent ratio shown in Fig. 1 should be a result of the interference of other surface species formed by solvent and salt reactions which compete with $Li_2CO_3$ formation and thus 'spoil' the Li passivation.

The high Li-cycling efficiency measured with DEC solutions under $CO_2$ should be understood as follows. Both DEC and MF reduction products are partly soluble in their mother solutions. Therefore, solvent reduction in this case does not interfere with $Li_2CO_3$ formation since this is the only species which is stable on the electrode's surface in DEC–MF–$CO_2$ solutions. Thus,

the $Li_2CO_3$ film in these cases is homogeneous and highly protective.

Cases such as MF–THF or MF–DMC solutions in which a minimum in Li-cycling efficiency is obtained as a function of the co-solvent concentration (Fig. 1) may be explained as follows. When the concentration of the two solvents is high, both contribute considerably to the build-up of the surface films (in addition to $Li_2CO_3$ formation). Therefore, the interphase formed on the Li is heterogeneous in its chemical composition and less protective.

The detrimental effect of $LiBF_4$ on Li-cycling efficiency measured in this work is also understood in light of the high reactivity of this salt anion as reflected by the surface spectroscopy (Fig. 10).

## 5. Conclusions

Mixtures of MF with ethers and alkyl carbonates, with $LiAsF_6$ as the electrolyte containing $CO_2$, may be suitable for use in secondary Li batteries with Li metal anodes. The key component in these solutions is $CO_2$ whose reaction on the Li surface forms $Li_2CO_3$ (and CO gas as a co-product [3,10]), which is an excellent passivating agent. Although Li deposition in $CO_2$ solutions is dendritic, the dendrites formed are properly protected by the inorganic carbonate and their corrosion is thus avoided. In contrast to other researchers' results obtained with cells of practical configuration [1,2], the effect of $LiBF_4$ on Li-cycling efficiency in MF solutions measured in this work is detrimental because of its high reactivity on the Li surface. It is assumed, however, that the pressure on the Li surface exerted by the separator in practical cells largely decreases detrimental effects of undesirable surface chemistry which induces 'rough' morphology of Li deposition.

## References

[1] E. Peled, C. Menachem, A. Gorenshtein and A. Alkon, in S. Surampudi and V. Koch (eds.), *Proc. Symposium on Lithium Batteries*, The Electrochemical Society Softbound Series, Proc. Vol. 93-24, The Electrochemical Society, Pennington, NJ, USA, 1993.

[2] E. Plichta, S. Slane, M. Vchiyama, M. Salomon, D. Chua, W.B. Ebner and H.W. Lin, *J. Electrochem. Soc., 136* (1989) 1865.

[3] Y. Ein-Eli and D. Aurbach, *Langmuir, 8* (1992) 1845.

[4] D. Aurbach and O. Chusid, *J. Electrochem. Soc., 140* (1993) L1.

[5] G. Nazri and R.H. Muller, *J. Electrochem. Soc., 132* (1985) 2050, 2054.

[6] D. Aurbach, Y. Ein-Eli and A. Zaban, *J. Electrochem. Soc., 141* (1994) L1.

[7] D. Aurbach and A. Zaban, *Proc. 7th Int. Meet. Lithium Batteries, Boston, MA, USA, May 1994,* in press.

[8] D. Aurbach, Y. Gofer and Y. Langzam, *J. Electrochem. Soc., 136* (1989) 3198.

[9] D. Aurbach, M.L. Daroux, P. Faguy and E.B. Yeager, *J. Electroanal. Chem., 297* (1991) 225.

[10] D. Aurbach, Y. Gofer, M. Ben-Zion and P. Aped, *J. Electroanal. Chem., 339* (1992) 451.

[11] D. Aurbach, M.L. Daroux, P. Faguy and E.B. Yeager, *J. Electrochem. Soc., 135* (1988) 1863.

[12] D. Aurbach, M.L. Daroux, P. Faguy and E.B. Yeager, *J. Electrochem., Soc., 134* (1987) 1611.

[13] D.P. Wilkinson, H. Blom, K. Brandt and D. Wainwright, *J. Power Sources, 36* (1991) 517.

[14] T. Hirai, I. Yoshimatsu and J.I. Yamaki, *J. Electrochem. Soc., 141* (1994) 611.